Effect of Pressure on Flow Parameters in Vertical Upwards Gas-Liquid Two-Phase Plug Flow

Masao NAKAZATOMI*, Hideo SHIMIZU*, Tumoru OCHIAI* and Yasuhide KAKUNO*

Abstract

This study investigated the pressure effects on the behaviors of gas and liquid slugs in vertical upward two-phase plug flow regime. The system pressure was changed from 0.3 to 20 MPa at a constant fluid (air-water) temperature. Measurements were carried out of the mean amplitude of liquid slugs, mean length of gas and liquid slugs, and liquid holdup around the gas slug. An empirical equation was also presented for the conditions under which the liquid slugs disappear.

Key Words: Pressure effect, Liquid slug, Gas slug, Disappearance of liquid slug

1. INTRODUCTION

A number of investigations on the flow parameters of gas-liquid two-phase plug flow have been reported so far both analytically and experimentally[(1)-(8)]. These works discussed on the effects of the flow rates and physical properties of both phases, flow direction, test section geometries and phase change. However the accumulated knowledge is still poorly limited and much has been left to be known to get insight into the physical mechanisms of gas-liquid two-phase flows. More efforts and investigations in this area are therefore indispensable.

Specifically the influence of the system pressure on the flow parameters characteristic in the plug flow region of an air-water two-phase flow has been insufficiently investigated until now. The flow parameters to be discussed in this report include the frequency and length of liquid slugs, the gas slug length and the liquid holdup around the gas slugs. The mean velocity of the liquid lumps and the average liquid holdup have been previously discussed in detail[(9)]. These parameters are characteristic features of the plug flow and are closely related to heat transfer mechanisms. In the plug flow region, the disappearance of the liquid slugs is also important because it causes a change in the liquid phase transport mechanisms. Sekoguchi et al.[(10)-(12)] have analyzed the behavior of liquid lumps in detail, and suggested that the disappearance of liquid slugs follows a transition from the froth flow to a region with huge waves.

The present report describes the experimental results of the influence of the system pressure on the primary flow parameters mentioned above. It also presents a criterion for the disappearance of the

* 宇部工業高等専門学校制御情報工学科

liquid slugs, based on the observations, to calculate the flow structures. The range of the system pressure covered in this work is 0.3~20 MPa.

2. NOMENCLATURE

D: tube inner diameter m,mm
Fr_G: Froud number $=j_G/(g \cdot D)^{1/2}$
g: acceleration of gravity m/s^2
h_p: fluctuation amplitude of static pressure difference mm in H_2O
j: superficial velocity m/s
j_{GV}: superficial gas velocity at minimum liquid holdup m/s
L: length m
m: natural logarithm of gas-liquid density ratio $=\ln(\rho_L/\rho_G)$
n: frequency Hz
P: pressure MPa
Re_{Lo}: liquid Reynolds number $=j_L \cdot D/\nu$
t: time sec
We: Weber number $=\rho_L \cdot j_L{}^2 \cdot D/\sigma$
η: liquid holdup
ν: kinematic viscosity m^2/s
ρ: density kg/m^3
σ: surface tension N/m

Subscripts
G: gas phase Gs : gas slug L : liquid phase
Ls: liquid slug $\overline{\ }$: mean value

3. EXPERIMENTAL APPARATUS AND PROCEDURE

The experimental arrangements used in this work are basically the same as those reported previously[9]. Figure 1 shows a schematic of the vertical test section made of a 10.4 m long stainless steel tube with 19.2 mm inside diameter. The viewing section was located at a position 5.4 m downstream of the air-water mixer.

The air was introduced into the water flow (tap water) through the 3 mm diam. holes drilled in a staggered lattice with 15 mm distance on the tube wall over an axial length of 110 mm (eight holes along the tube perimeter times four lines in axial direction).

For local void fraction measurements, a point electrode probe was inserted into the flow at a distance of 6 m downstream from the test section inlet. The pressure taps were equipped at three axial positions at intervals of 0.5 m to measure the local pressures. The wall conductance probe technique was used to measure the liquid holdup downstream of each pressure taps.

The following parameters specifying the plug flow structures were measured in the present work; time-varying cross-sectional averaged liquid holdup $\overline{\eta}$, mean length $\overline{L}_{Ls}$ and frequency $\overline{n}_{Ls}$ of the liquid slugs, the mean length of the gas slugs $\overline{L}_{Gs}$ and mean velocity of the liquid lumps; radial distribution of the local void fraction ; static pressure and pressure gradient.

Experimental conditions covered in this work were as follows : superficial water velocity $j_L=0.010\sim0.50$m/s, superficial air velocity $j_G=0.06\sim10$ m/s, pressure $P=0.30\sim20.0$ MPa, with corresponding air-water density ratio (ρ_G/ρ_L) ranging from 0.0034 to 0.225, fluid temperature $\theta=28\sim32$ ℃.

The frequency and length of the liquid slug, and length of the gas slug were obtained from time-varying cross-sectional averaged liquid holdup signals.

4. RESULTS AND DISCUSSION

4.1. Photographic observation and time-varying cross-sectional averaged liquid holdup

Photo 1 shows the slug flow taken at the axial position 5.4 m downstream from the air-water mixer. Photo (a)~(e) correspond to the pressure condition P=0.3, 5, 10, 15 and 20 MPa, respectively. As can be seen in this photo many small bubbles are distributed in the liquid slug almost uniformly at pressures higher than 5 MPa. So, the gas slug absorbs many small bubbles from the movement of the liquid slug and produces many small bubbles in its wake.

The time-varying cross-sectional averaged liquid holdup η is an important characteristic to determine the structure of the liquid lumps. Figure 2 shows the time-varying character of η for a 10 sec duration at different gas velocities $j_G=0.2$, 0.3, 0.4, 0.5, 0.55, 0.6, 0.65, 0.7, 0.8, 1.0 and 1.5 m/s (P=20 MPa and $j_L=0.3$ m/s). The convexity in the η-curves corresponds to the liquid slugs or waves on the residual liquid film between the gas slug and the wall and gas core. It is recognized from Fig. 2 that the liquid slugs disappear at j_G between 0.65 and 1.0 m/s.

4.2. Mean frequency of liquid slug

Figure 3 shows the relation between the mean frequency of the liquid slug passing $\bar{n}_{Ls}$ and the superficial gas velocity j_G at pressures P=10 and 20 MPa with the liquid velocity j_L being a parameter. The broken lines in the figure represent plots of the point where form a minimum point on the liquid holdup line, and is calculated by Eq.(1)[9].

$$Fr_G=j_{Gv}/(g\cdot D)^{1/2}=7.40We^{0.1}\exp(1.30\times10^{-6}Re_{Lo}-2.55)\cdot m \tag{1}$$

where D is the tube diameter, We the Weber number ($=\rho_L\cdot j_L^2\cdot D/\sigma$), Re_{Lo} the liquid Reynolds number ($=j_LD/\nu_L$) and m is the logarithmic gas-liquid density ratio ($=\ln(\rho_L/\rho_G)$).

From these plots the mean frequency $\bar{n}_{Ls}$ are divided into two characteristic regions separated by the afore mentioned broken line for constant j_L. In region I $\bar{n}_{Ls}$ holds a near constant value under a small j_G, while in region II $\bar{n}_{Ls}$ decreases rapidly to zero with an increase of j_G. The symbols on the horizontal coordinate in Figs. 3(a) and 3(b) show the points of $\bar{n}_{Ls}=0$. The boundary between the regions I and II is physically interpreted as a point where the liquid slug frequency begins to rapidly decrease, despite a change in the system pressure and flow rate ofboth phases j_G and j_L[9].

As is seen in Fig.3, $\bar{n}_{Ls}$ increase with an increase of j_L in the region I and it shifts to large j_G in the region II. The condition is thus determined as the intersection of j_G where the liquid slugs disappear of $\bar{n}_{Ls}$ with the horizontal coordinate, i.e., $\bar{n}_{Ls}=0$. The qualitative changes of $\bar{n}_{Ls}$ with j_G and j_L show the same tendency at other pressures.

Figure 4 shows the relation between $\bar{n}_{Ls}$ and j_G for various pressures for $j_L=0.10$ m/s. The symbols denoted on the horizontal coordinate correspond to $\bar{n}_{Ls}=0$. For small j_G the value $\bar{n}_{Ls}$ shows no systematic dependence on j_G, being nealy at constant. However, in the region II, it is dramatically affected by the system pressure and shifts towards small j_G with an increase in pressure. Similar trends were observed for different values of j_L. The effect of gas-liquid density ratio on $\bar{n}_{Ls}$ is thus remarkable in the region II.

As mentioned earlier, the value of $\bar{n}_{Ls}$ in the region I show almost constant values and are unaffected by the system pressure. These pressure-independent constant values of $\bar{n}_{Ls}$ are approximated by the following empirical equation;

$$\bar{n}_{Ls}=0.5\ \{(e^{1.55j_L}-0.4)+(4.2j_L{}^{0.424})\} \tag{2}$$

Equation (2) is shown by a solid line in figure 4. The applicability of Eq.(2) is as follows : $P=0.3\sim20$ MPa, $j_L=0.010\sim0.503$ m/s, $j_G=0.06\sim j_{Gmax}$, where j_{Gmax} is given by Eq.(1).

4.3. Mean length of liquid and gas slugs

Figure 5 shows the relation between $\bar{L}_{Ls}$ and j_G. The boundary between regions I and II is also shown in the figure by a dashed line. Experimental conditions are the same as in the case of Fig.3(a). The relation shows that $\bar{L}_{Ls}$ has an almost constant value of 0.2~0.3 with slight variations in the region of small j_G. For j_G larger than 0.4 m/s, $\bar{L}_{Ls}$ reaches maximum values with an increase of j_G. Then it decreases rapidly. On the other hand with an increase of j_L, the $\bar{L}_{Ls}$ curve generally shifts to a larger j_G.

This result coincides with a rapid decrease of $\bar{n}_{Ls}$ for an increase of j_G (refer to Fig.3(a)), which follows a change in the liquid transport process caused by the transition from the liquid slugs to the liquid film and waves. In the region where $\bar{L}_{Ls}$ increases, the collapse of the liquid slug has already begun (a rapid decrease of $\bar{n}_{Ls}$), followed by the coalescence of the two liquid lumps and, therefore, $\bar{L}_{Ls}$ increases and supplements the liquid flow rate. Similar trends were observed in $\bar{L}_{Ls}$ vs. j_G curves at different pressures . This has been confirmed also by the needle probe placed at the tube center.

Figure 6 shows the relation between $\bar{L}_{Gs}$ and j_G. The experimental conditions are the same as in the case of Fig.3(a). In this figure the broken line indicates the boundary between the regions I and II. The value $\bar{L}_{Gs}$ increases with an increase of j_G. However, no clear differencecan be seen in the trend between the two regions. By increasing j_L, $\bar{L}_{Gs}$ generally shifts to larger j_G. The similar trends were obtained at different pressures.

In the region I, these data compaier fairly well with the correlation[13], (symbol ● in Fig. 6) originally obtained at atomospheric pressure. However both in the transition region from the region I to the region II, and in the region II, the predicted values are smaller than the experimental data.

Figure 7 shows the effect of the system pressure on the $\bar{L}_{Gs}$ and j_G diagram at $j_L=0.10$ m/s. The correlation(13) for $P=0.1$ MPa is also represented in this figure by the long broken line. As is clear from this figure, no systematic effect of the system pressure was observed in the region of $j_G<0.3$ m/s. For $j_G\geqq0.3$ m/s, the pressure effect is clearly seen and $\bar{L}_{Gs}$ increases as j_G approaches to the region II. In the region II, this trend becomes more remarkable. This is followed by the fact that the disappearance of liquid slugs shifts toward smaller j_G with an increase in the system pressure as can be seen in Fig. 4.

4.4. Liquid holdup around gas slug

At near atmospheric pressures, the liquid film around the gas slug in the region I is rather smooth.

But in the case of $P \geqq 5$ MPa, the gas slug interface is accompanied by ephemeral large waves [9] and thus the instantaneous liquid holdup varies with time.

Figure 8 shows the experimental results of the time averaged liquid holdup $\overline{\eta}_{Gs}$ around gas slugs versus the superficial gas velocity j_G. The time averaged liquid holdup $\overline{\eta}$ after the disappearance of liquid slugs is plotted also in the figure with a dotted line.

In the region I, $\overline{\eta}_{Gs}$ shows a decreasing trend with an increase of j_G at small j_G, and then increases at larger j_G near the region II. $\overline{\eta}_{Gs}$ increases also with j_L systematically in the region I. However, near the boundary between the regions I and II, no systematic variation of $\overline{\eta}_{Gs}$ is no longer observed.

Whereas in the region II, $\overline{\eta}_{Gs}$ increases rapidly with an increase of j_G. On the $\overline{\eta}$-curves in this region, the liquid lumps (i.e. ephemeral large wave and huge wave) increase rapidly[9]. The velocity of these liquid lumps are slower than that of the liquid slugs. It is therefore considered that in this region $\overline{\eta}_{Gs}$ increases with a decrease of $\overline{n}_{Ls}$. As for $\overline{\eta}$ in the region II, it has a maximum at a certain value of j_G and as indicated by dotted line. The boundary between the regions I and II exists in general very close to this maximum point. However, $\overline{\eta}_{Gs}$ does not indicate such clear trends.

The disappearance of liquid slugs are indicated by the symbol ↓ in Fig. 8. From the figure, the existence of liquid slugs is no longer found at j_G where $\overline{\eta}$ shows a maximum point. The liquid slug disappears at j_G just before the $\overline{\eta}$ curve forms a maximum point.

The $\overline{\eta}$ curve decreases rapidly after forming a maximum value with an increase of j_G. In other words, the behavior of the $\overline{\eta}$ curve indicates a decrease in film thickness. Similar trends were observed for different the system pressures.

Figure 9 shows the pressure dependence of $\overline{\eta}_{Gs}$ and j_G diagram at $j_L = 0.10$ m/s. An increase in the pressure is to increase $\overline{\eta}_{Gs}$ at constant j_G. Especially, the value of j_G where the liquid slugs disappear (symbol: ↓ in the figure) clearly shifts towards a smaller j_G with an increase in pressure.

4.5. Disappearance of liquid slug

The characteristic tendencies of $\overline{n}_{Ls}$, $\overline{L}_{Ls}$, $\overline{L}_{Gs}$ and $\overline{\eta}_{Gs}$ againist the change of the velocities of both phases and system pressure have been discussed in the previous paragraphs. These flow parameters are related to the disappearance of liquid slugs, which has been determined based on the following observations.

① In Figs. 3(a), 3(b) and 4, n_{Ls} in the region II decreases rapidly toward zero with an increase in j_G.

② As shown in Figs. 8 and 9, $\overline{\eta}_{Gs}$ in the region II has the $\overline{\eta}$-maximum point. Immediately before this maximum point was reached, the liquid slug disappeared.

③ The oscillation amplitude of the static pressure difference h_p was a characteristic behavior with j_G at the point of the disappearance of liquid slugs as shown in Fig.10.

The h_p increases generally with an increase of j_G, and then decreases rapidly at a certain value of j_G. This value of j_G coincides with the conditions determined by the methods described in ① and ②. This has been confirmed from the flow pattern observation[9] and also from the time-dependent $\overline{\eta}$ -value (for time interval 180 sec). In Fig.10 the symbol ← shows the disappearance of liquid slugs.

On the basis of these results, Eq.(3) is proposed for the value of j_G at the disappearance of liquid slugs.

$$Fr_G = 5.6We^{0.05}\exp(0.34\times10^{-4}\ Re_{Lo}\cdot m^{0.32}-2.31)\ m^{1.35} \quad (3)$$

where $m = \ln(\rho_L/\rho_G)$.

Figure 11 shows the comparison of Eq.(3) with experiments. The application limits of Eq.(3) are : $P=0.3\sim20$ MPa, $j_L=0.010\sim0.503$ m/s, D=19.2mm.

5. CONCLUSIONS

Several important flow parameters characterizing the plug flow region in a vertically upward air-water two-phase flow in a round tube were investigated experimentally at the system pressure ranging from 0.3 to 20 MPa. The results obtained are as follows:

(1) The liquid slug frequency showed two distinct characteristic regions. Region I: mean frequency shows a near constant value. Region II: mean frequency decreases rapidly and reaches zero with an increase of the superficial gas velocity.

(2) The empirical correlation has been presented for the region I.

(3) The mean length of the liquid slug in the region I obtained in this study was the order of magnitude about $0.2\sim0.3$ m. The influence of the system pressure in the region I is minimal. In the region II, the liquid slug disappeared just before the mean length reached its maximum at $0.4\sim0.5$ m. This characteristic was commonly observed at all pressures.

(4) The liquid holdup $\overline{\eta}_{Gs}$ around the gas slug shows different tendencies in the regions I and II. In the region I, $\overline{\eta}_{Gs}$ at small superficial gas velocity j_G, decreased with an increase of j_G. In the region II, however, it increased rapidly with an increase of j_G, and then reached a maximum (similarly in the $\overline{L}_{Ls}$-j_G diagram). At this point, the liquid slug has already disappeared.

(5) An empirical correlation has been proposed to predict the conditions of liquid slugs disappearance.

Acknowledgement—The authors express their thanks to Messors M. Taniguchi and Y. Hisatomi for fabricate up the test section. The authors also gratefully acknowledge the support from the special grant in aid for the scientific research from the ministry of Science, Education and Culture, Japan.

REFERENCES

(1) Griffith, P. and Wallis, G.B., Two-Phase Slug Flow. *Trans. ASME* Ser. C, 83,(1961), 307-320.

(2) Akagawa, K. and Sakaguchi, T., Fluctuation Characteristics of Void Fraction in Gas-Liquid Two-Phase Flow (4th Report, Bubble Distribution). *Trans.Jap.Soc.Mech.Engrs*, 31,(1965), 608. (In Japanese).

(3) Street, J.R. and Tek, M.R., Unsteady State Gas-Liquid Slug Flow through Vertical Pipe. *AIChE. J.*, 11,(1965), 601-605.

(4) Fukano, T., Sekoguchi, K. and Nishikawa, K., Length of Gas Slug and Liquid Slug in Gas-Liquid Two-Phase Flow. *Technol. Repts. Kyushu Univ.*, 46,(1973), 144-151. (In Japanese).

(5) Laird, A.D.K. and Chisholm, D., Pressure and Forces along Cylindrical Bubbles in a Vertical Tube. *I & EC*. 48,(1956), 1361-1364.

(6) Ozgu, M.R., Chen, J.C. and Stenning, A.H., Local Liquid Film Thickness around Taylor Bubbles. *Trans. ASME, J. Heat Transfer*, Ser. C, 95,(1973), 425-427.

(7) Ozgu, M.R., and Chen, J.C., Local Film Thickness during Transient Voiding of a Liquid Filled Channel. *ASME Paper*, WA-HT-27, (1975).

(8) Fukano, T., Matumura, K., Kawakami, Y. and Sekoguchi, K., Unsteady State Phenomenon in Two-Phase Slug Flow (2nd Report, Liquid Film Thickness around Gas Slug). *Trans.Jap.Soc. Mech.Engrs,* 46,(1980), 2412-2419. (*In Japanese*).

(9) *Sekoguchi, K., Nakazatomi, M., Takeishi, M., Shimizu, H., Mori, K. and Miyake, J., Pressure Effect on Velocity of Liquid Lumps in Vertical Upward Gas-Liquid Two-Phase Flow. JSME Int. J*. Series II, 35, (1992), 380-387.

(10) Sekoguchi, K., Takeishi, M., Hironaga, K. and Nishiura, T., Velocity Measurements with Electrical Double-Sensing Devices in Two-Phase Flow. *IUTAM Symp., Measuring Techniques in Gas-Liquid Two-Phase Flow*,(1984), 455-477, Springer, Berlin.

(11) Sekoguchi, K., Takeishi,M. and Ishimatsu, T., Interfacial Structure in Vertical Upward Annular Flow. *Physico-Chem. Hydrodynamics*. 6,(1985), 239-255.

(12) Sekoguchi, K. and Takeishi, M., Interfacial Structures in Upward Huge Wave Flow and Annular Flow Regimes. *Int. J. Multiphase Flow* 15,(1989), 295-305.

(13) Sekoguchi,K.,*Gas-Liquid Two-Phase Flow. Progress of Heat Transfer Engineering*, (1973), 282. Yokendo Publishing Co., (In Japanese).

(平成6年9月20日受理)

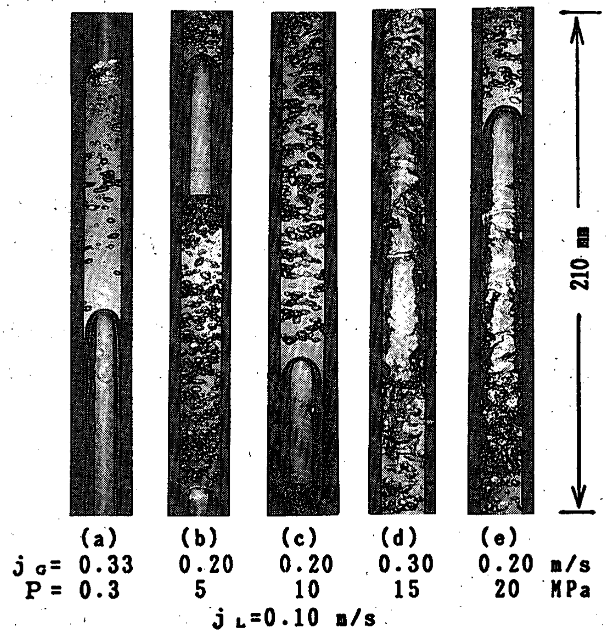

Photo 1. Typical photograph of the flow regimes.

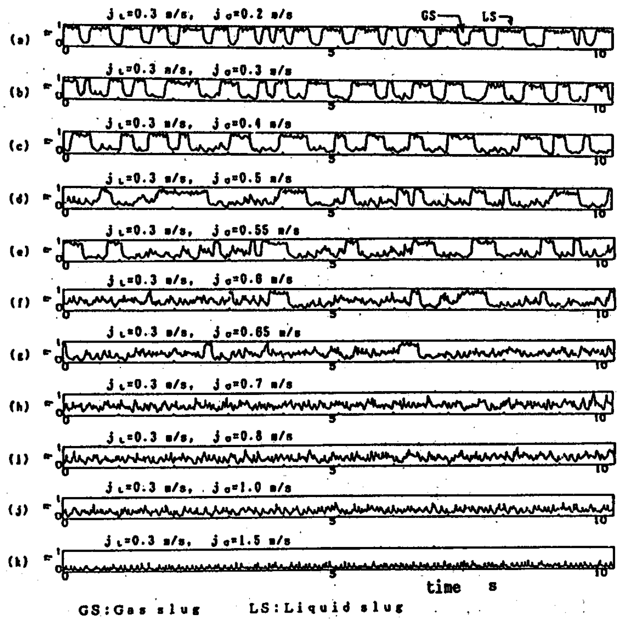

Figure 2. Time-varying cross-sectional liquid holdup signals, P=20 MPa.

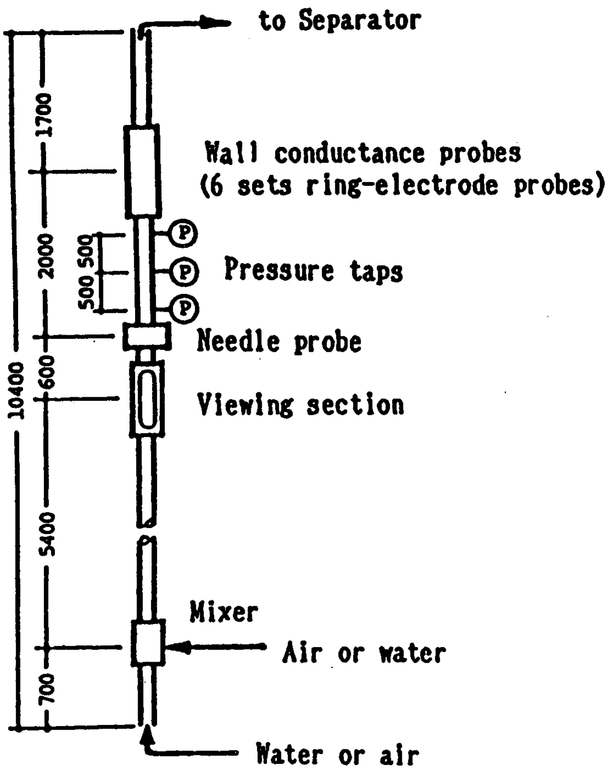

Figure 1. A schematic diagram of the test section.

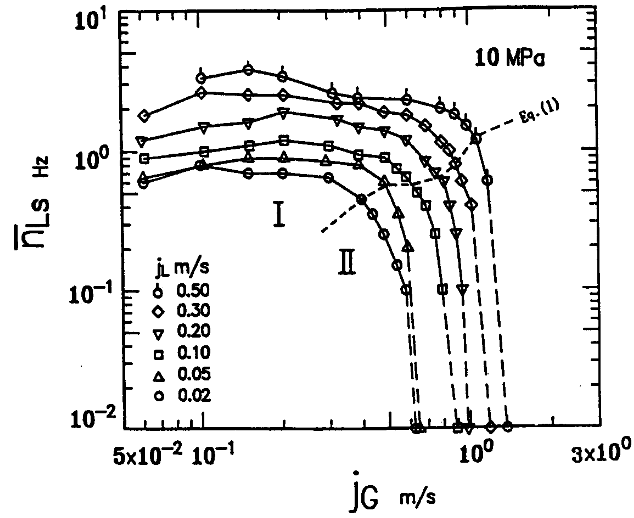

Figure 3(a). Mean frequency of liquid slug $\overline{n}_{LS}$. (Symbols on the horizontal coordinate show the points of $\overline{n}_{LS}=0$).

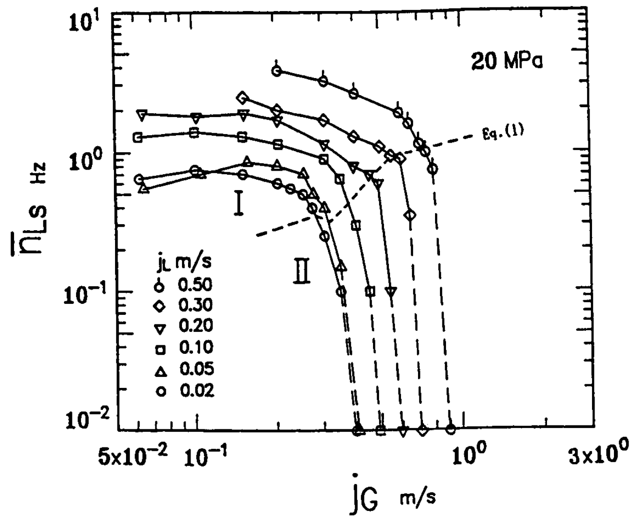

Figure 3(b).

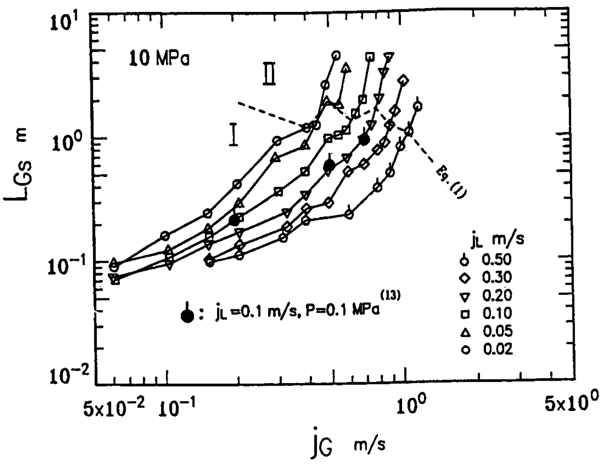

Figure 6. Mean length of gas slug $\overline{L}_{GS}$.

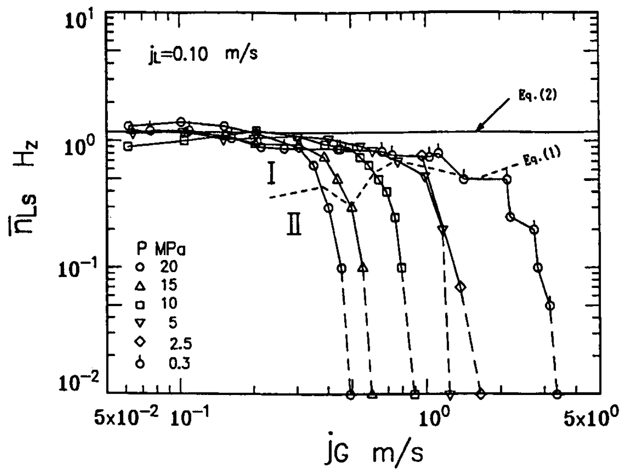

Figure 4. Pressure effect on the mean frequency of liquid slug $\overline{n}_{LS}$. (Symbols on the horizontal coordinate show the points of $\overline{n}_{LS}=0$).

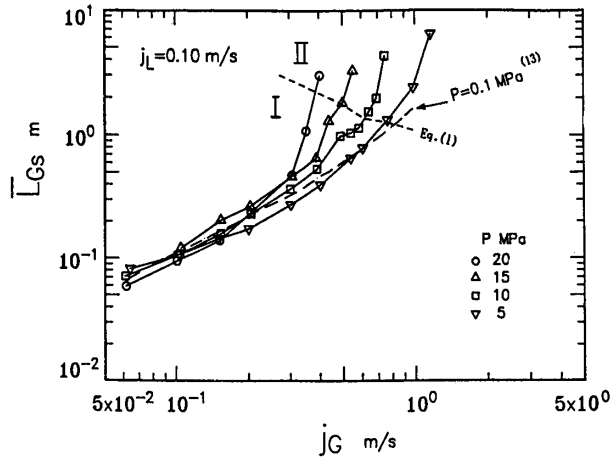

Figure 7. Pressure effect on the mean length of gas slug $\overline{L}_{GS}$.

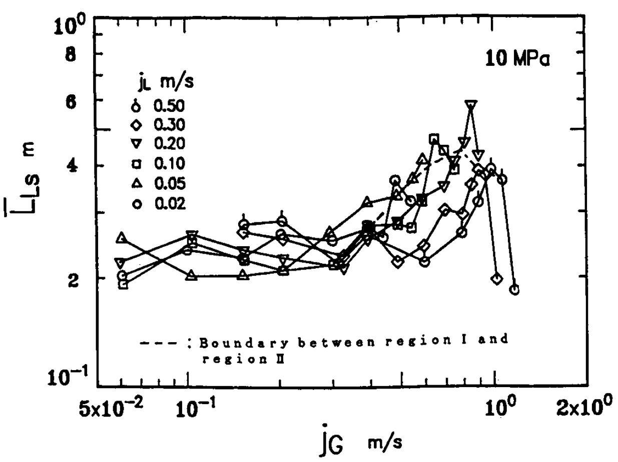

Figure 5. Mean length of liquid slug $\overline{L}_{LS}$.

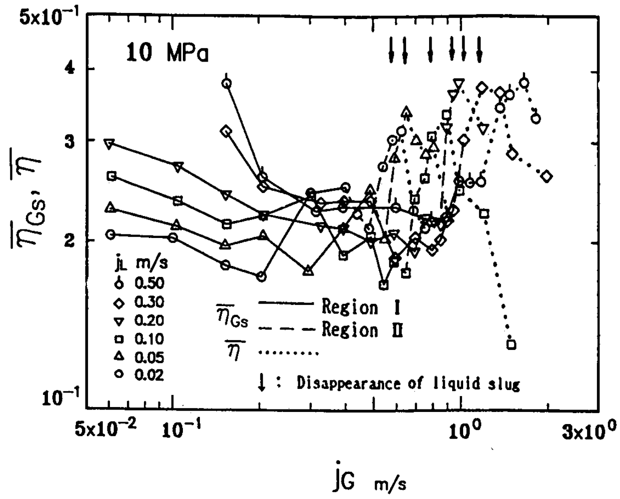

Figure 8. Liquid holdup around the gas slug $\overline{\eta}_{GS}$.

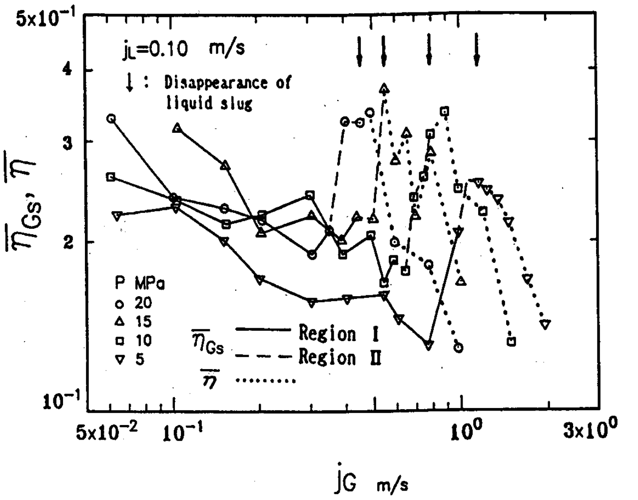

Figure 9. Pressure effect on the liquid holdup around the gas slug η_{Gs}.

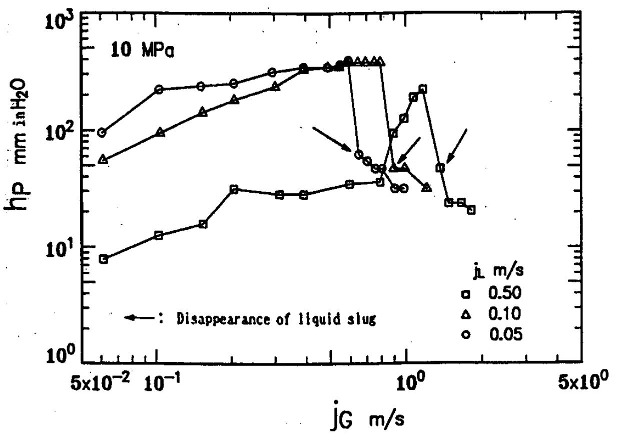

Figure 10. Fluctuation amplitude of the static pressure difference h_p.

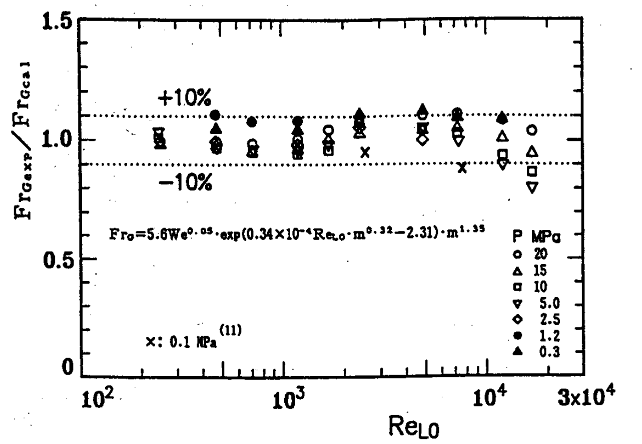

Figure 11. Comparison of Eq.(3) with experimental data for the disappearance of liquid slugs.